https://rbgeomorfologia.org.br/
ISSN 2236-5664

Revista Brasileira de Geomorfologia

v. 27, nº 2 (2026)

https://dx.doi.org/10.20502/rbg.v27i2.2687

Research Article

The impact of forest fires on sediment connectivity in the semiarid region

O impacto de incêndios florestais na conectividade de sedimentos no semiárido

Felipe de Lima Brito [1], Jonas Otaviano Praça de Souza [2] e Ellen Luana Brasilino Lemos Madeiro [3]

[1] Universidade Federal da Paraíba, Departamento de Geociências, João Pessoa, Brasil. E-mail: felipeGeo_Acad@outlook.com ORCID: https://orcid.org/0009-0007-8738-0753

[2] Universidade Federal da Paraíba, Departamento de Geociências, João Pessoa, Brasil. E-mail: jonas.souza@academico.ufpb.com.br ORCID: https://orcid.org/0000-0002-1405-0944

[3] Universidade Federal da Paraíba, Departamento de Geociências, João Pessoa, Brasil. E-mail: ellen.madeiro@academico.ufpb.br ORCID: https://orcid.org/0009-0008-8809-4406

Received: 03/03/2025; Accepted: 24/04/2026; Published: 14/06/2026

Abstract: Forest fires, intensified by human activities, are transformed into environmental disasters and affect biomes that are not naturally adapted to fire, such as the Caatinga. With the advent of climate change and the increasing number of fires, it becomes necessary to understand their impact on surface environmental dynamics, including sedimentological processes. One way to analyze these changes is through sediment connectivity, which refers to the physical linkages that enable the potential transfer of sediments across the landscape. Therefore, this study aims to analyze the impacts of fire through sediment connectivity, using remote sensing imagery from before and after the fire events and applying connectivity and vegetation indices. The results show a 14% increase in connectivity values in the study area, which is proportional to the fire's intensity. Vegetation indices indicate a slow recovery of the area. Finally, limitations were observed in the use of proposed roughness input values for burned areas, as well as in the natural recovery capacity of the Caatinga, which, even after four years, had not returned to pre-fire levels.

Keywords: Connectivity Index; NDVI; Wildfires Severity; Caatinga.

Resumo: Os incêndios florestais, potencializados pelas ações humanas, são transformados em desastres ambientais e afetam biomas que não são naturalmente adaptados ao fogo, como no caso da caatinga. Com o advento das mudanças climáticas e o aumento da quantidade de incêndios, surge a necessidade de entender qual o impacto deles na dinâmica ambiental superficial, incluindo a dinâmica sedimentológica. Umas das maneiras de analisar essas mudanças é através da conectividade sedimentológica, que pode ser explicada como as ligações físicas para a potencial transferência de sedimentos ao longo da paisagem. Sendo assim, o presente trabalho tem como objetivo analisar os impactos de incêndio a partir da conectividade sedimentológica, através de análises de imagens de sensoriamento remoto de antes e depois dos incêndios e da aplicação de índices de conectividade e vegetação. Os resultados mostram um aumento de 14% nos valores de conectividade na área estudada sendo proporcionais ao nível de intensidade do fogo. Os índices de vegetação mostram lenta recuperação da área. Por último, foram observadas as limitações da utilização dos valores de entrada da rugosidade propostos para incêndios e na capacidade de recuperação natural da caatinga, que após quatro anos não retornaram a níveis pré-incêndios.

Palavras-chave: Índice de conectividade; NDVI; severidade de incêndios; Caatinga.

1. Introduction

The Brazilian semiarid region covers 900,000 km², encompassing the states of the Brazilian Northeast and municipalities in northern Minas Gerais. Like the rest of the world, it has been experiencing changes in environmental dynamics; one of these is the increase in forest fires, predominantly caused by anthropogenic activities (Santana et al., 2011).

The increasing frequency and intensity of forest fires, driven by human actions, are evolving into environmental disasters and affecting biomes, including those that are not naturally fire-adapted, such as the Caatinga. These fires can alter natural landscape dynamics, affecting vegetation, soil, and water availability (Hallema et al., 2017; López-Vicente, Kramer, & Keesstra, 2021a). With climate change and the consequent potential for increased fire frequency and magnitude, there is a need to understand their impact on environmental dynamics. In the Caatinga, few studies have examined the relationship between fires and impacts on erosion patterns, although the impacts of fires have long been recognized in the international literature.

The impacts of fires on environmental dynamics can be chemical and physical, with chemical phenomena preceding physical ones. The former is related to changes in the chemical properties of soil and biomass due to high temperatures, which transform the uppermost layer into a sealing, impermeable layer, in addition to transforming the canopy and leaf litter into ash (Redin et al., 2011). Physical changes resulting from soil sealing and canopy removal reduce infiltration capacity and, consequently, increase runoff and sediment transport capacity. The formation of an ash layer on the soil increases water retention capacity; however, it saturates quickly and is not continuous (Redin et al., 2011).

To analyze sedimentological dynamics, it is necessary to understand the physical environmental system, defined as a set of components (forms, mass, energy, and events) interconnected by flows of matter and energy (Phillips, 2012). Christofoletti (2002) presents the "physical environmental system" as synonymous with the geosystem and the object of analysis in Physical Geography. At the same time, it is necessary to use an appropriate spatial scale for systemic analysis, such as the drainage basin, described by Coelho Neto (1998, p. 95) as areas of the earth's surface that drain water, sediments, and dissolved materials to a common outlet at a specific point in a river channel.

In the study of systems, it is crucial to understand the relationship between matter, energy, and structure. Matter corresponds to the material mobilized within the system; energy is represented by the force (potential or kinetic) that enables the system to perform work; and structure relates to the elements, their relationships, and the spatial/temporal arrangement of the system's components (Christofoletti, 1979; Souza, 2013).

In drylands—comprising dry sub-humid, semiarid, and arid areas (aridity index below 0.65) (Middleton; Sternberg, 2013)—these relationships are directly linked to rainfall patterns and seasonality. It is important to note that, even in drylands, surface dynamics are controlled by rainfall, as in the Brazilian semiarid region (Carvalho, 2020; Hastenrath, 2012). Thus, rivers in the semiarid region are predominantly non-perennial, with continuous flow for most of the year. Channels that flow only during precipitation events are ephemeral rivers, while those that maintain flow throughout the rainy season are called intermittent rivers (Souza and Almeida, 2015).

At the same time, seasonal precipitation dynamics directly affect the predominant biome of the Brazilian semiarid, the Caatinga. Classified as a seasonally dry neotropical forest, it is typical of vegetation located in areas with high evapotranspiration (1,500 – 2,000 mm/year), low precipitation (300 – 1,000 mm/year), and fertile, slightly acidic soils (Dryflor, 2016; Lima et al., 2018a). Precipitation is the primary controller of its deciduous/semi-deciduous behavior, with biomass varying between levels close to Savannah (NDVI ± 0.2) and those close to Humid Forests (NDVI ± 0.8) (Fernandes et al., 2022; Souza; Hooke, 2021).

These impacts on sedimentological dynamics can be analyzed using the sediment connectivity approach, defined as the physical links for the potential transfer of sediment from one area to another through the channel (Hooke, 2001). Seasonality affects connectivity—a theoretical concept ideal for geomorphic studies that originated in ecology to define the transport of matter, energy, and organisms through water (López-Vicente; González-Romero; Lucas-Borja, 2020a). The term was first used in fluvial analysis to determine which parts of the fluvial system are connected. Sediment connectivity, specifically, is the water-driven transport of soil and sediment across the landscape, which can be measured by the relationship between the sediment source and the locations of temporary or permanent deposition (Hooke, 2003).

The hillslope, as a sediment source, differs from the channel in its dynamics and controllers. This relationship is referred to as lateral linkages, in which sediment transport is linked to slope stability and mass movements. The main controllers of these dynamics are slope gradient and morphology, geology, vegetation, animals, and anthropogenic activities (Brierley; Fryirs; Jain, 2006; Lu et al., 2019).

Thus, connectivity is primarily controlled by the rainfall-runoff relationship, which ultimately dictates the behavior of ephemeral and intermittent rivers (Souza; Hooke, 2021). Connectivity in the semiarid can be further divided into hillslope processes and fluvial processes. On hillslopes, vegetation density and land use are the main flow controllers; in fluvial environments, flow occurs during floods in ephemeral rivers and is influenced by the alluvial water table level. This rainfall dynamic and its influence on vegetation produce high levels of surface runoff and, consequently, higher connectivity rates (Souza; Almeida, 2015).

Identifying connectivity patterns after extreme events is useful for communities both near and far from burned areas. Decreased water availability and flooding are possible consequences, underscoring the need for local communities to understand the impacts of fires, which can cause sudden changes in local connectivity.

These changes can be evaluated using vegetation, fire, and connectivity indices. A very common vegetation index is the NDVI (Normalized Difference Vegetation Index), which uses red and near-infrared bands to measure vegetation's spectral response at a given time. For fire analysis, a common index is the NBR (Normalized Burn Ratio), which uses near-infrared and shortwave infrared bands to identify burned areas and estimate severity. Lastly, the connectivity index helps in understanding sediment transport behavior.

The present study aims to analyze the impacts of a fire in the semiarid region based on sediment connectivity. To achieve this, pre- and post-fire remote sensing imagery will be used, and indices of fire severity and lateral hydrological connectivity will be applied.

2. Study area

The study area is in the municipality of Floresta, in the semiarid region of Pernambuco, and is delimited by three different sub-basins: the Riacho Aretas basin to the south, and the Riacho Toco do Pau and Pedra Branca basins to the north, which are part of the Riacho do Navio sub-basin (Figure 2). The area was affected by a fire (Figure 1) between November 4 and 9, 2019, covering approximately 29 km².

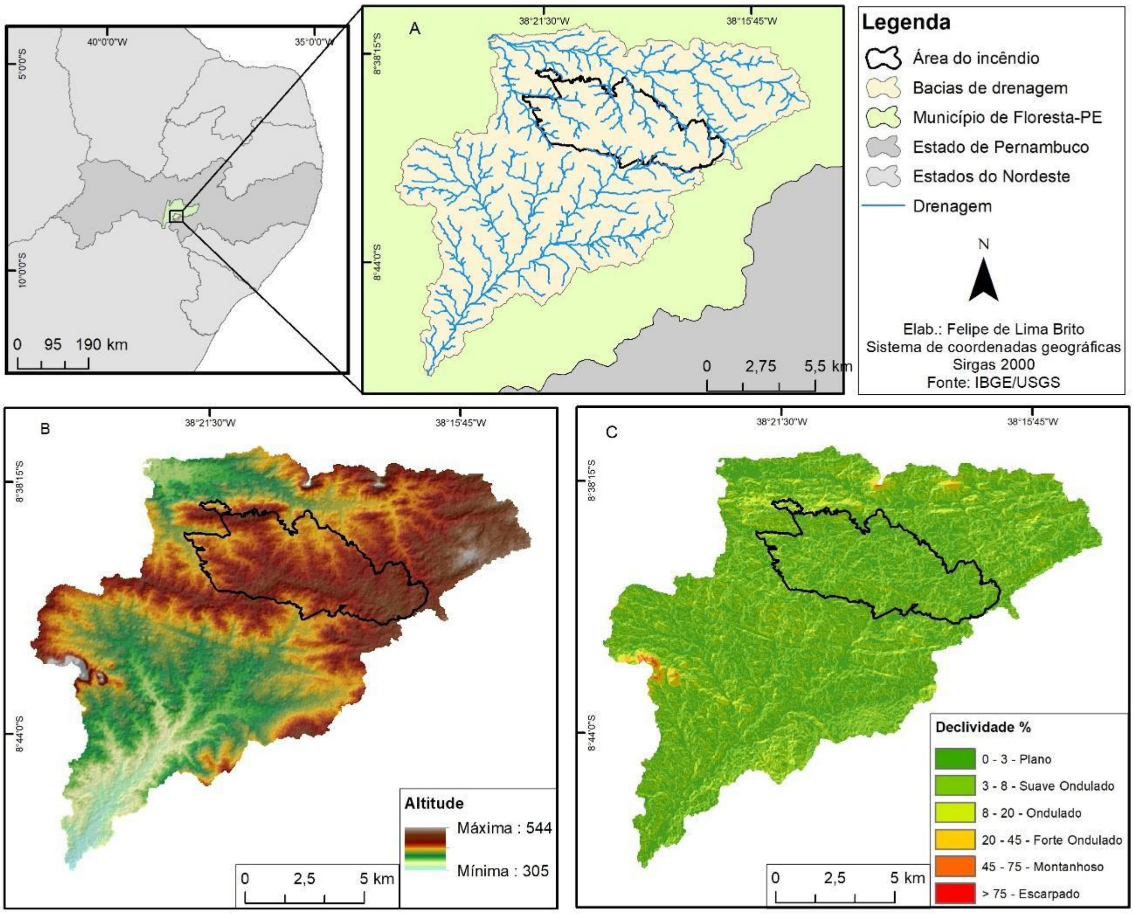

Figure 1. Mosaic with the location maps (A), digital elevation model (DEM) (B), and slope (C).

The area features altitudes ranging from 358 to 414m, with an altimetric amplitude (or relief range) of 56m. While slope values are predominantly low, between 0 and 8% across most of the area, only a few sections exceed 8%. The geological substrate consists of metamorphic rocks, specifically gneiss and orthogneiss from the Belém do São Francisco complex.

According to MAPBIOMAS data (Figure 2), the majority of the study area is composed of savanna and grassland formations, which are addressed in this text as dense shrubby Caatinga and sparse shrubby Caatinga. Some stretches consist of agriculture and pasture, data which were validated through fieldwork on November 25, 2023. Furthermore, the area lies within the boundaries of three sub-basins: the Riacho Aretas basin to the south, and the Riacho Toco do Pau and Pedra Branca basins to the north, both of which are part of the Riacho do Navio sub-basin (Figure 2).

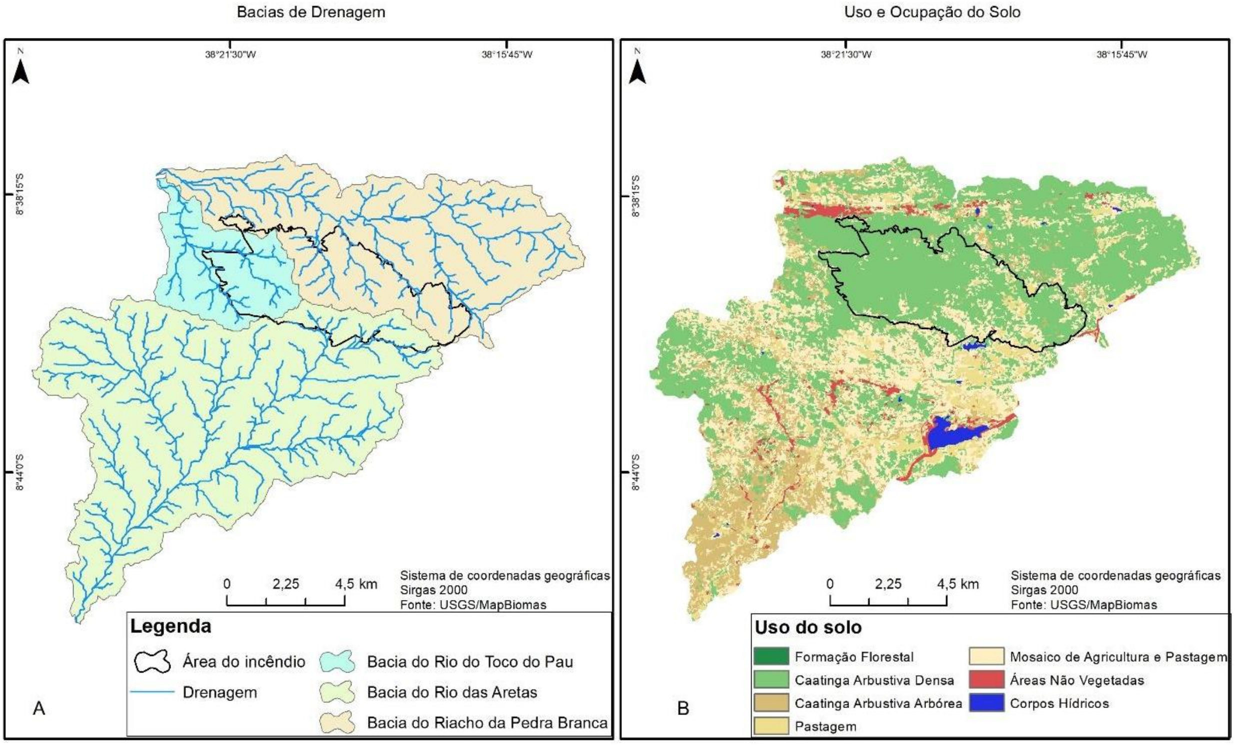

Figure 2. (A) Mosaic with the drainage basin maps; (B) land use and land cover.

Annual rainfall within the analyzed period ranged from **800mm in 2010** to approximately **125mm in 2012**. The sample average reached **462mm**, while extreme events (**exceeding 50mm**) occurred in 24 of the 28 years analyzed.

Graph 1. Mosaic of graphs showing annual rainfall totals, extreme events, and monthly averages.

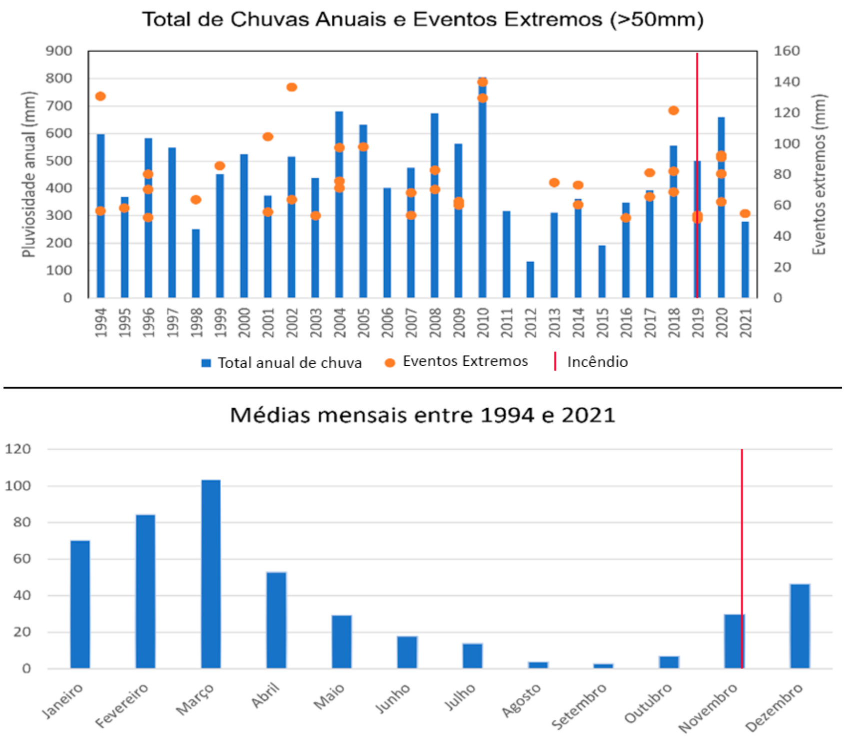

During the event period, from November 4 to 9, 2019, no rainfall events were recorded. The total precipitation for the entire month of November was 36mm, occurring on November 26, 17 days after the fire.

The highest monthly averages occur between January and March, with the latter exceeding 100mm. The lowest averages are found in August and September, reaching approximately 4mm.

3. Materials and methods

To obtain the Digital Elevation Model (DEM), SRTM (Shuttle Radar Topography Mission) imagery at 30-meter resolution was used. Data on the burned area were obtained from images acquired by the OLI sensor on the Landsat 8 satellite, provided by the United States Geological Survey (USGS), with a 30-meter spatial resolution. Following the methodology proposed by Key and Benson (2006), pre-fire (10/31/2019) and post-fire (11/16/2019) images were collected. Subsequently, the fire area was delimited using the Normalized Burn Ratio (NBR) - Eq. (1) (Key; Benson, 2006) and delta NBR (dNBR) - Eq. (2) (Parks; Dillon; Miller, 2014).

$$\text{NBR} = \frac{(\mathbf{B5}-\mathbf{B7})}{(\mathbf{B5}+\mathbf{B7})} \tag{1}$$

$$dNBR = \left(NBR_{(pre-fogo)}\right) - \left(NBR_{(pós-fogo)}\right) \tag{2}$$

For the NBR, near-infrared (B5) and shortwave infrared 2 (B7) bands are used. These specific bands are chosen because they exhibit opposing responses to fire: while B5 tends to show a decrease in reflectance after a fire, B7 shows an increase.

The delta NBR (dNBR) is used to identify fire severity in the area by calculating the difference between the pre-fire NBR and post-fire NBR. To classify this intensity, supervised classification and the minimum distance algorithm within ArcMap 10.8 software were employed.

Fire severity was assessed using dNBR to improve data precision across spatial scales (Miller and Thode, 2007; Martini et al., 2020). Land-use mapping was obtained from the MAPBIOMAS Collection 7, with a spatial resolution of 30 meters. This collection uses the mean of images over the year, resulting in more consistent and representative results across different periods.

To calculate the connectivity index, the SedInConnect v2.3 software (Crema; Cavalli, 2018) was used, applying Eq. (3) as proposed by Borselli et al. (2008). This formula relates the upslope component (numerator) to the downslope component (denominator). Values range from -∞ to +∞ , where lower values indicate a lower capacity of the environment to generate surface runoff and a reduced connection between the sediment-producing area and the fluvial channel.

$$IC = log_{10}\left(\frac{\omega \times s \times \sqrt{A}}{\sum \frac{d}{W \times s}}\right) \tag{3}$$

The elements present in the numerator of Equation 3 are: "ω", representing the surface roughness resistance (in this case, values related to the C-factor); "s", the mean slope of the contributing area (m/m); and "A", representing the contributing area (m^2). The denominator estimates the sediment travel distance using the following data: "W", the land cover coefficient; "S", the slope (m/m); and "d", the distance to the main drainage.

The W-index (presented in Table 1) ranges from 0.001 to 1 and corresponds to the soil roughness index, used to estimate the influence of land cover on hydrological connectivity and sediment transport. This index is essential for understanding how different types of vegetation cover interfere with surface runoff dynamics.

Lower W values (closer to 0) are associated with high-roughness surfaces, such as densely vegetated areas, where natural cover acts as a barrier to flow. It reduces water velocity, promotes higher infiltration, and consequently decreases hydrological connectivity.

In contrast, higher **W values** (closer to 1) indicate low roughness, typical of exposed, deforested, or urbanized surfaces. In these locations, the absence of cover elements allows greater accumulation and surface movement of water, favoring **concentrated flow** and increasing the potential for erosion and sediment transport (Ortíz-Rodríguez; Muñoz-Robles; Borselli, 2019a).

Table 1. W values. Source: adapted from Ortíz-Rodríguez et al. (2009a) and Montes-Leon et al. (2011).

Formação Florestal	0.001
Caatinga Arbustiva Esparsa	0.045
Caatinga Arbustiva Densa	0.040
Pastagem	0.150
Mosaico de Agricultura e Pastagem	0.125
Outras Áreas Não Vegetadas	0.900
Incêndios de Alta Severidade	0.950
Incêndios de Média Severidade	0.056
Incêndios de Baixa Severidade	0.001

To obtain the "W" values, the parameters established by Ortíz-Rodríguez et al. (2019) were used, with distinct values for land use and land cover areas and for areas affected by fire. These produce lower values for areas with low fire severity and higher values for areas with greater severity. It is important to emphasize that this is an indirect approach based on conceptual models.

To understand the impacts of fire on vegetation response, Landsat-8 (OLI sensor) and CBERS 4A (WPM sensor) satellites were used, specifically the red (B3) and near-infrared (B4) bands, with resolutions of 30 and 8 meters, respectively. The Normalized Difference Vegetation Index (NDVI) - Eq. (4) was applied to these images.

$$NDVI = \frac{(B5-B4)}{(B5+B4)} \quad (4)$$

Using rainfall data for the municipality of Floresta - PE, obtained from the ANA (National Water Agency) website for station A351, it was possible to generate graphs for average monthly rainfall, total annual rainfall, and the occurrence of extreme events (Graph 1). These events, defined as exceeding 50mm, were analyzed between 1994 and 2021.

4. Results and Discussion

Land-use data provided by MAPBIOMAS for 2019 and 2020 (Figure 3) show virtually no difference between the years. These variations may even be attributed to errors within the measurement instruments and/or the methodology itself. The area known to have been affected by the 2019 fire shows no type of alteration in these data. According to MAPBIOMAS, the estimated overall accuracy for Collection 7.1 in the Caatinga biome is 77.1%; meanwhile, Souza et al. (2020) reported accuracy levels across the entire Caatinga ranging from 78.18% to 80.03%.

Table 2 presents the land-use values in km² and percentages obtained from the MAPBIOMAS imagery. The variation between the images reaches a maximum of 0.98% for pasture use and -0.97% for the mosaic of agriculture and pasture category. These variations do not reflect the fire, which affected an area of 29.1 km².

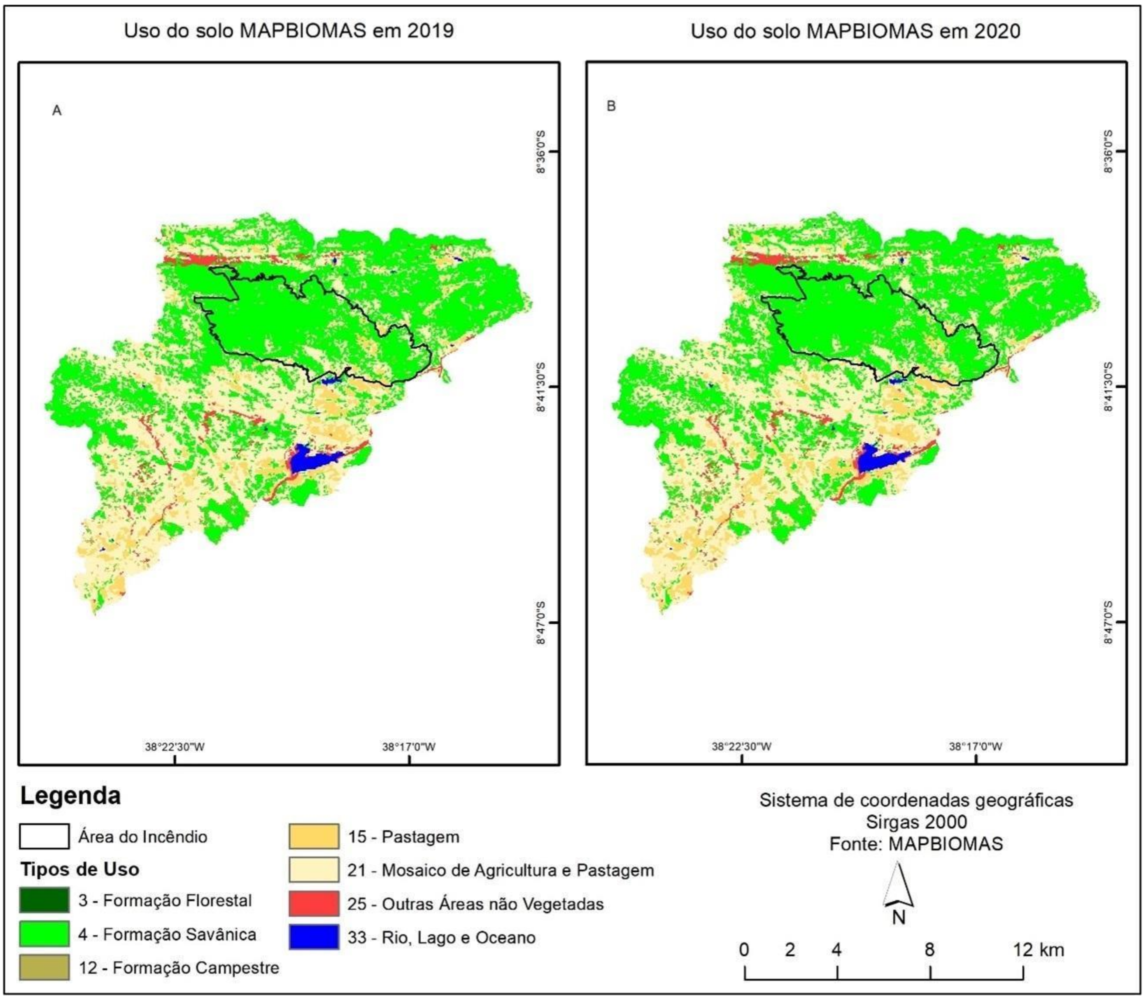

Figure 3. (A) Mosaic showing land use and land cover in 2019 and (B) 2020.

Table 2. Land use data for the entire basin from the 2019 and 2020 MAPBIOMAS imagery.

Uso do Solo 2019			Uso do Solo 2020			Diferença	
Tipo de Uso	Area km²	%	Tipo de Uso	Area km²	%	Área km²	%
Formação Florestal	0,0126	0,01%	Formação Florestal	0,0135	0,01%	0,0009	0,00%
Formação Savanica	86,9031	47,89%	Formação Savanica	86,9724	47,93%	0,0693	0,04%
Formação Campestre	1,9044	1,05%	Formação Campestre	1,9089	1,05%	0,0045	0,00%
Pastagem	13,0977	7,22%	Pastagem	14,868	8,19%	1,7703	0,98%
Mosaico de Agricultura e Pastagem	73,3446	40,42%	Mosaico de Agricultura e Pastagem	71,5932	39,45%	-1,7514	-0,97%
Outras Áreas Não Vegetadas	4,4964	2,48%	Outras Áreas Não Vegetadas	4,4865	2,47%	-0,0099	-0,01%
Rio, Lago e Oceano	1,7112	0,94%	Rio, Lago e Oceano	1,6272	0,90%	-0,084	-0,05%
Total	181,47	100%	Total	181,47	100%		

The images generated from the NBR (Normalized Burn Ratio) and dNBR (delta Normalized Burn Ratio) indices, presented in Figure 4, clearly show the changes in vegetation resulting from the analyzed fire event. The NBR index, used to identify areas affected by fire by comparing near-infrared and shortwave infrared bands, showed pre-event values ranging between 0.42 and -0.19. These values indicate a predominantly healthy vegetation cover, with few degraded areas. However, after the event, the minimum NBR values dropped to -0.28, suggesting a significant loss of vegetation and, therefore, a direct impact from the environmental disturbance.

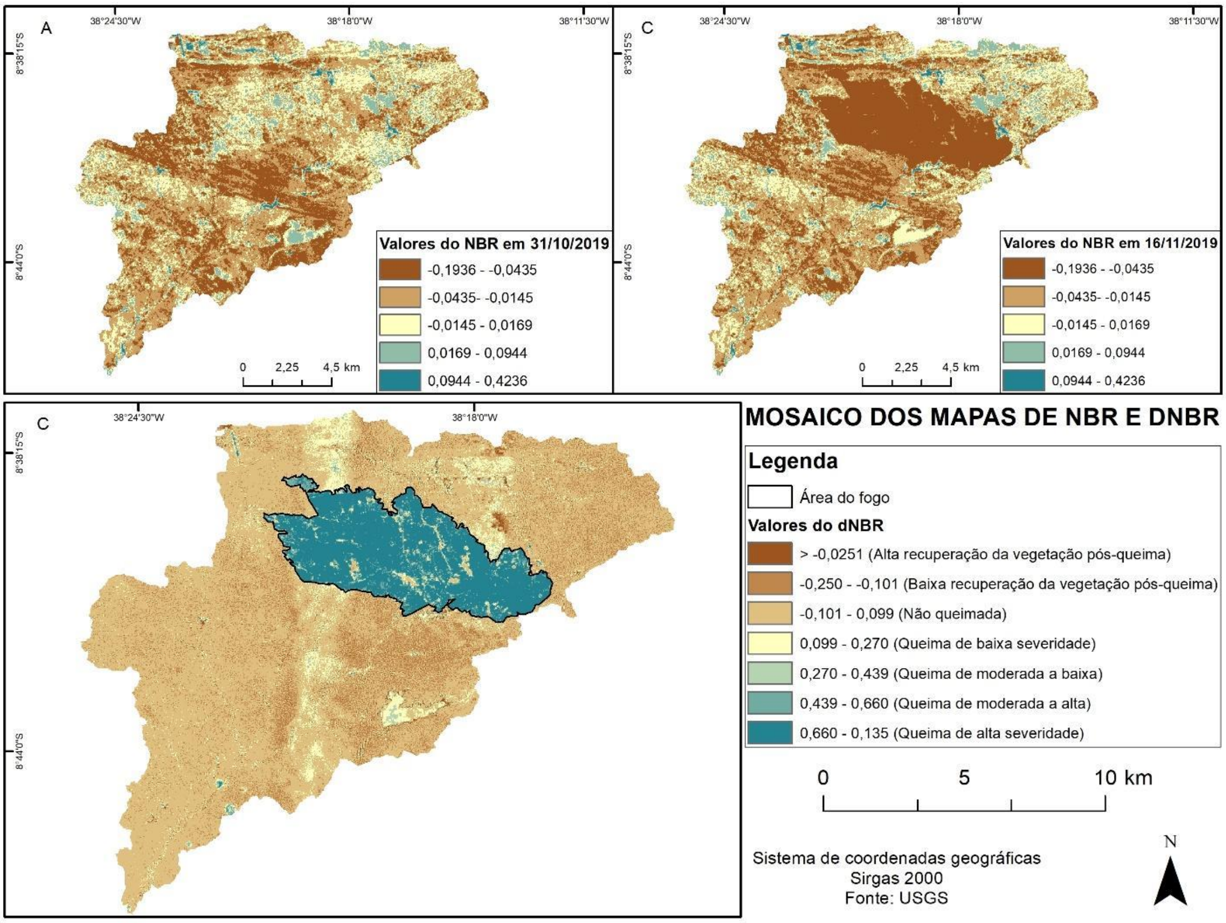

Figure 4. (A) Mosaic of the NBR for 10/31/2019 – pre-fire, (B) 11/16/2019 – post-fire, and (C) dNBR.

These values are also used to estimate fire severity, with moderate and high intensities represented by positive values. According to Key and Benson (2006), these represent the burned areas. The severity estimation was also based on the values proposed by the USGS FireMon program.

After estimating fire severity, the land-use values of the basin before and after the event were compared, along with their differences (Table 3). The primary land uses identified were dense shrubby Caatinga (47.97%), mosaic of agriculture and pasture (40.62%), and pasture only (7.11%).

Table 3. Land use values before and after the fire.

Valores Pré Incêndio			Valores Pós Incêndio			Diferença Entre Pós-Pré	
Tipo de Uso do Solo	Área Km²	%	Tipo de Uso do Solo	Área Km²	%	Área Km²	%
Formação Florestal	0,01	0,01%	Formação Florestal	0,01	0,01%	0	0,00%
Caatinga Arbustiva Densa	87,15	47,97%	Caatinga Arbustiva Densa	64,4	35,45%	-22,75	-12,52%
Caatinga Arbustiva Esparsa	1,73	0,95%	Caatinga Arbustiva Esparsa	1,53	0,84%	-0,2	-0,11%
Pastagem	12,92	7,11%	Pastagem	11,92	6,56%	-1	-0,55%
Mosaico de Agricultura e Pastagem	73,79	40,62%	Mosaico de Agricultura e Pastagem	68,7	37,82%	-5,09	-2,80%
Outras Áreas Não Vegetadas	4,36	2,40%	Outras Áreas Não Vegetadas	4,36	2,40%	0	0,00%
Água	1,7	0,94%	Água	1,7	0,94%	0	0,00%
			Incêndios de Alta Severidade	17,54	9,66%	17,54	9,66%
			Incêndios de Média Severidade	11,5	6,33%	11,5	6,33%
Total	181,66	100%	Total	181,66	100%		

Post-fire values changed by 15.99%, directly related to the fire. Of this total, 9.66% were classified as high severity and 6.33% as moderate severity. The land use category that experienced the greatest reduction was dense shrubby Caatinga (12.52%), which is explained by its predominance within the actual fire area.

This observation is particularly important, as the most intense fires occurred within the dense, shrubby Caatinga (Figure 5). In contrast, agriculture and pasture mosaics and non-vegetated areas exhibited lower severity. It can be explained by the fact that grasses provide less fuel and have a lower calorific value than trees and shrubs.

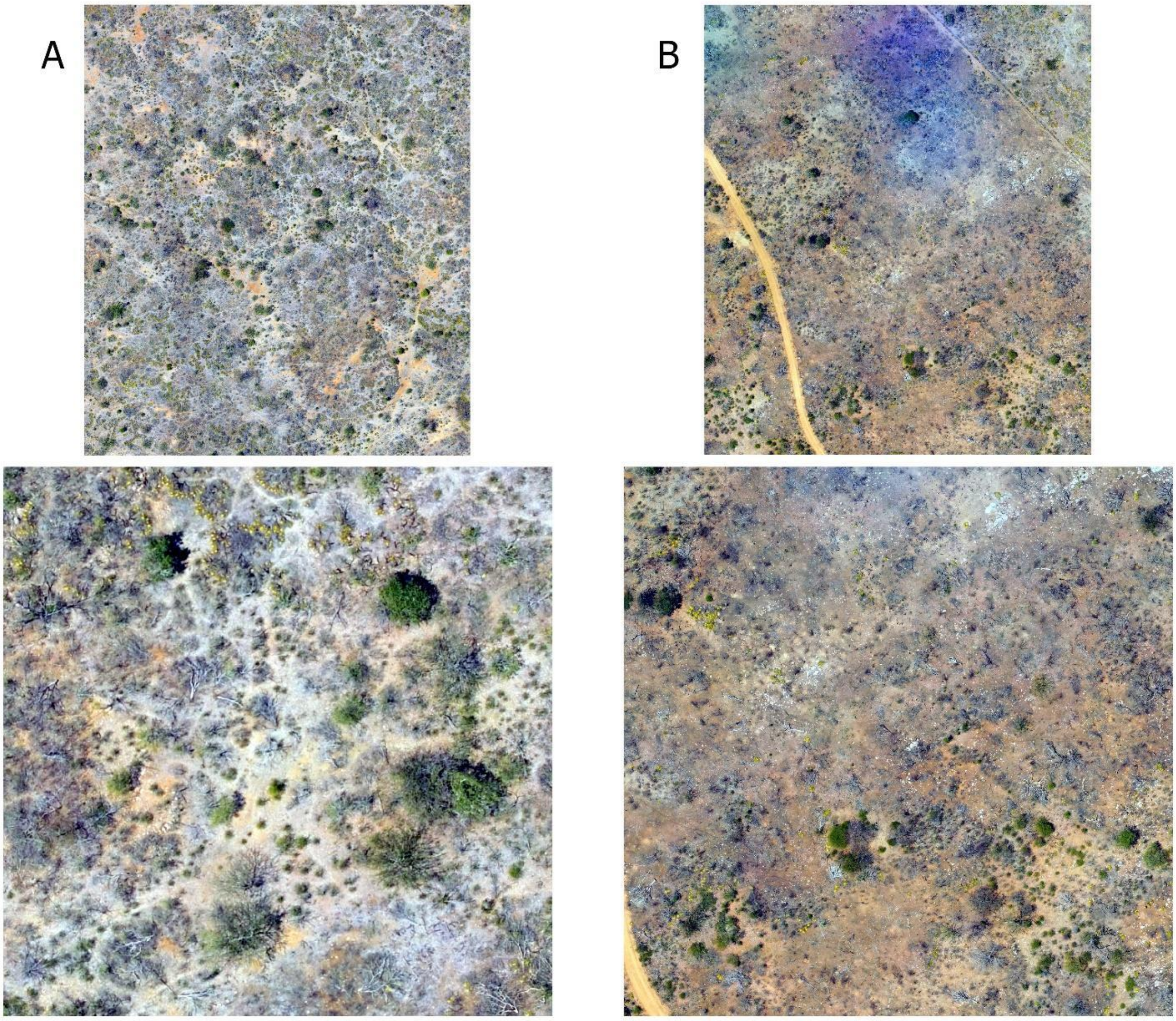

Figure 5. (A) Mosaic showing the locations of moderate-severity fires and (B) high-severity fires in 2022.

The direct relationship between fire severity and areas with denser shrub-tree cover is a determining factor in the connectivity index results, as they present the largest difference (0.905) in the input data (W).

As expected, connectivity values tend to increase following the event. While the minimum values of the connectivity index remain stable, there is a considerable rise in the higher values, with a 14% increase in maximum values after the event (Table 4). The average connectivity values increased as the range of results widened, as demonstrated by the increase in standard deviation.

Table 4. Minimum, maximum, and mean connectivity values, and standard deviation.

	Mínimo	Máximo	Média	Desvio Padrão
IC pré incêndio	-11,978	1,7118	-7,8715	0,7104
IC pós incêndio	-11,978	1,9626	-7,7012	0,7801

Corroborating the trend are the values obtained by calculating the difference between the post- and pre-event periods, which show little to no variation across all areas—except for the fire zone. In contrast, the regions affected by the fire exhibit the greatest differences, reaching peaks of 2.96 (Figure 6), precisely where dense shrubby vegetation was removed due to high fire severity.

The eastern portion of the area was most affected by severe fires, resulting in the greatest reduction of the vegetation canopy. Additionally, natural factors of xerophytic vegetation, such as the absence of leaf cover before the rainy season, aggravated this condition. The impact on the soil was also significant, as the area consists of a Chromic Luvisol with high clay content, making it more susceptible to soil sealing, especially in areas hit by high-intensity fires (Stavi, 2019).

The results for the hydrological connectivity index indicate a trend toward increased connectivity in fire-affected areas, similar to those reported by Martínez-Murillo and López-Vicente (2016) and Ortíz-Rodríguez et al. (2019a). The quantity, potential calorific value, and continuous distribution of fuel are factors that control fire intensity.

No rainfall occurred between the dates of satellite data acquisition. The nearest event occurred on November 27, 17 days after the fire (Graph 2), impacting areas that had likely undergone canopy removal and remobilizing fire-derived debris, including charcoal and ash, as well as sediments. While the transport of unburned debris and ash can reduce downstream connectivity, it is not possible to assess this influence using remote sensing alone.

Graph 2. Precipitation 120 days after the event.

According to Souza and Hook (2021), landscape connectivity tends to increase, especially in degraded areas, as foliage recovery occurs. This regeneration process is particularly influenced by climatic conditions, being enhanced during the rainy season. Consequently, the observed increase in connectivity is even more significant during this period, highlighting rainfall as a driving factor in ecological restoration.

However, the removal of original vegetation, combined with the low fire-adaptation of certain biomes, significantly exacerbates the impacts of the rainy season. In contexts where fire acts as a disturbance agent, the loss of vegetation cover compromises soil infiltration capacity and increases susceptibility to erosion, intensifying the negative effects of heavy rains.

The impact of the rainy season was classified as extreme, as the months following the fire event—especially December, January, February, and March—recorded the highest average precipitation (as shown in Figure 3), along with the occurrence of extreme weather events. These factors acted on an already fragile area, where the capacity for foliage regeneration was limited, even during the period of greatest water availability.

Furthermore, the connectivity difference (Figure 6) shows that nearly the entire area affected by the fire presented positive changes, predominating over negative ones. Values close to zero are rare within the polygon, reinforcing the idea that a significant shift in the region's connectivity has occurred.

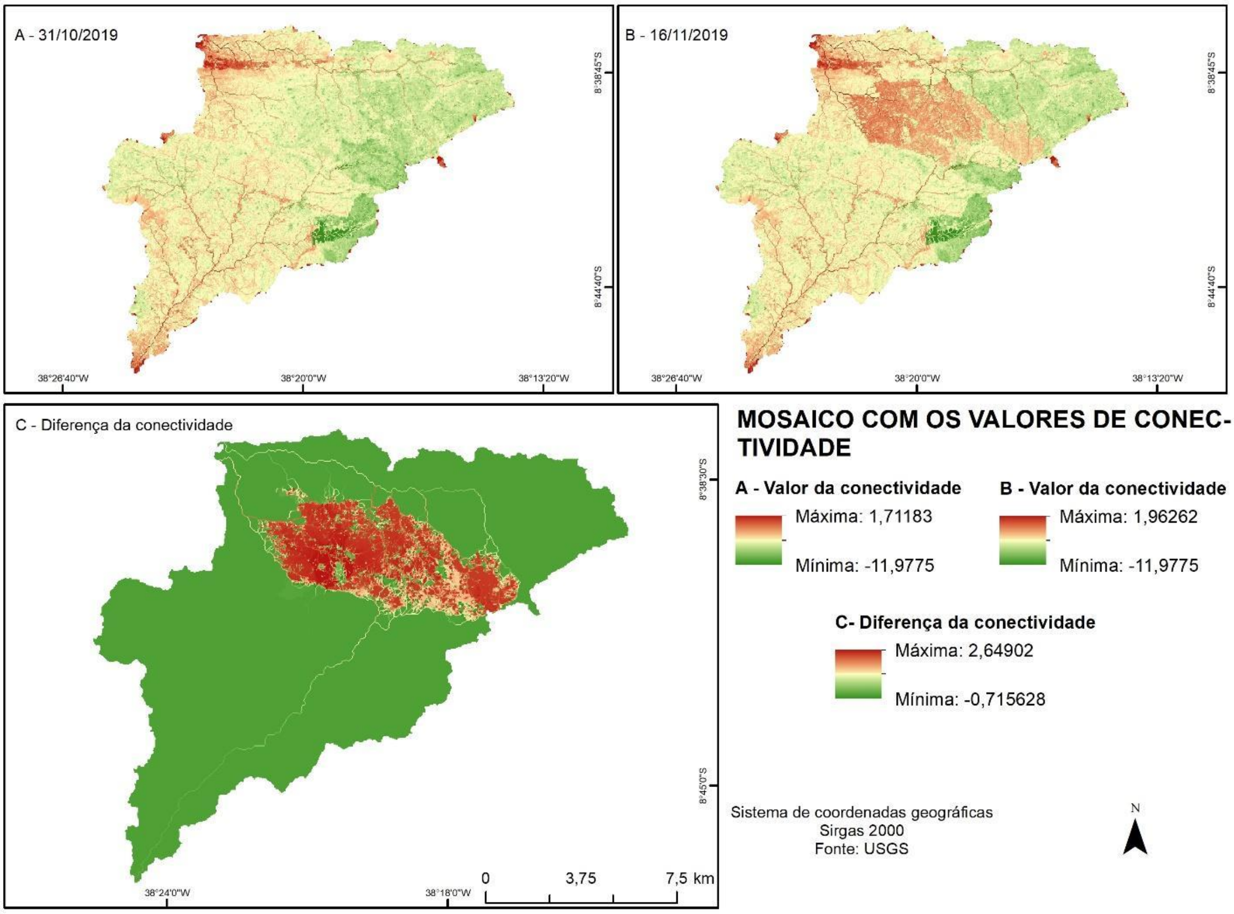

Figure 6. (A) Mosaic with connectivity values on 10/31/2019, (B) 11/16/2019, and (C) the result of the connectivity difference.

Figure 7 shows the NDVI results for the basin at three distinct moments: (A) immediately after the fire; (B) 9 months after the fire; and (C) 3 years after the fire. The results indicate vegetation recovery between 2019 and 2022, with an average increase of 7.61% and peaks of up to 24.55% in vegetation indices. However, areas that experienced the most intense fires showed a slower recovery rate.

This finding aligns with Sampaio (1998), who, in studying Caatinga recovery after removal with and without fire, demonstrated the difficulty of this vegetation in recovering from such impacts, particularly at higher intensities. In that study, even after six years, the Caatinga did not show the same individual density. However, species such as *Mimosa tenuiflora* (Jurema Preta) and *Bauhinia cheilantha* (Mororó) show faster responses to fire.

For comparison, the studies by Sampaio (1998) and Alves et al. (2013) demonstrate the natural recovery capacity of the Caatinga, with density values ranging from 25% to 40% of the original amount within 6 years. Although some recovery in tree density occurs, species diversity is reduced; Poincianella bracteosa (Catingueira), Croton sonderianus (Marmeleiro), and Bauhinia cheilantha (Mororó) are the species with the greatest recovery (Tarcisio, 2013).

When compared to burned areas, general species density does not exceed **15%** (**Sampaio, 1998**). This value varies according to fire intensity and the specific species' tendency to recover. In low and moderate-intensity fires,

Jurema Preta and **Catingueira** show the greatest increase in density. In high-intensity fires, the only species to increase in density is Mororó, reaching more than twice its initial density (**Sampaio, 1998**).

The higher NDVI values in 2023 (Figure 7, C) are due to higher rainfall rates in January and February. Within the fire polygon, values increased, likely due to grass resprouting, as reported by Sampaio (1998), yet remained well below those in the surrounding areas.

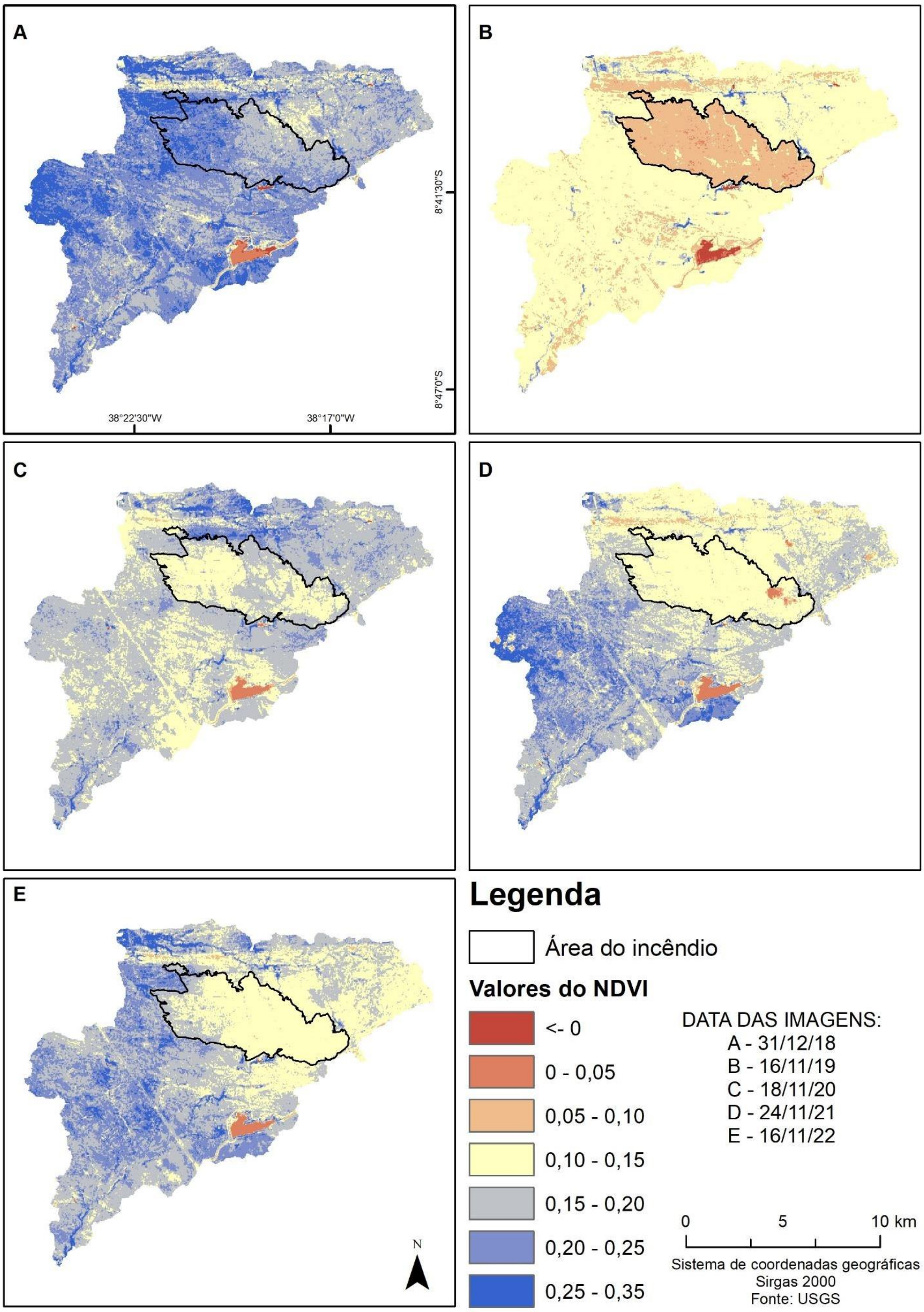

Figure 7. Mosaic with NDVI maps on (A) 12/31/2018, (B) 11/16/2019, (C) 11/18/2020, (D) 11/24/2021, and (E) 11/16/2022.

5. Conclusions

In the studied fire, moderate and high severities prevailed, which can be attributed to the high calorific value of the plants, the propagation speed, the high presence of dry biomass, and low rainfall.

The recovery capacity of the Caatinga in fire-affected areas is limited, as values had not returned to pre-fire levels four years after the event. Despite the scarcity of literature on this theme, the Caatinga recovery process tends to be slow, with difficult restoration of pre-fire conditions and a propensity to intensify desertification in affected areas.

Because of fire severity, connectivity values shifted across the entire polygon, generally trending toward increased connectivity. This study identified a limitation in the input values for the fire severity index, which were originally developed for continuous forests; for example, some land uses have surface roughness values higher than those for moderate-intensity fires. It is important to emphasize that post-fire recovery in the Caatinga is directly linked to increased roughness, which is one of the primary factors controlling surface hydro-geomorphological dynamics. Finally, monitoring recovery and surface roughness variation is essential, and UAVs (Unmanned Aerial Vehicles) offer a low-cost option for this.

Author Contributions: Conceptualization, F. L. B. and J. O. P. S.; methodology, F. L. B.; software, F. L. B.; validation, F. L. B. and J. O. P. S.; formal analysis, F. L. B.; research, F. L. B.; data curation, F. L. B.; writing—original draft preparation, F. L. B.; writing—review and editing, E. L. B. L. M.; supervision, X.X. All authors have read and agreed to the published version of the manuscript.

Funding: This research received no external funding.

Acknowledgments: The authors would like to thank the Semiarid Fluvial Environments Study Group (GEAFS).

Conflicts of Interest: The authors declare no conflict of interest.

References

1. ALMEIDA, C. P. A.; CAMPOS, J. R. D.; COSTA, A. C. S. Effects of fire on chemical and physical soil attributes in a *Cerrado sensu stricto* area. **Revista de Agrogeoambiental**, v. 13, n. esp. 2, 2021.
2. ALVES, J. M. B. et al. A Study of Heat Sources in the Caatinga Biome and their Relationships with Meteorological Variables. **Revista Brasileira de Meteorologia**, v. 36, n. 3, p. 513–527, 2021. DOI: 10.1590/0102-77863630015.
3. BOND, W. J.; KEANE, R. E. Fires, Ecological Effects of. In: ROITBERG, B. D. **Reference Module in Life Sciences**. 1st Ed. Elsevier, 2017. p. 1-11.
4. BORSELLI, L.; CASSI, P.; TORRI, D. Prolegomena to sediment and flow connectivity in the landscape: A GIS and field numerical assessment. **Catena**, v. 75, n. 3, p. 268–277, 2008. DOI: 10.1016/j.catena.2008.07.006.
5. BRIERLEY, G.; FRYIRS, K.; JAIN, V. Landscape connectivity: The geographic basis of geomorphic applications. **Area**, v. 38, n. 2, p. 165–174, 2006. DOI: 10.1111/j.1475-4762.2006.00671.x.
6. CARVALHO, A. T. F. Climatic characterization of the rainy season in a Brazilian semiarid municipality between 2013 and 2017. **Geografia em Atos (Online)**, v. 2, n. 17, p. 04–23, 2020. DOI: 10.35416/geoatos.v2i17.7116.
7. CHRISTOFOLETTI, A. **Modeling of Environmental Systems** (*Modelagem de Sistemas Ambientais*). 2nd Ed. São Paulo: Editora Edgard Blücher, 2002. 256p.
8. COELHO NETTO, A. L. Hillslope hydrology at the interface with geomorphology. In: GUERRA, A. J. T.: CUNHA, S. B. **Geomorphology: an update of bases and concepts**. 3rd Ed. Rio de Janeiro: Bertrand Brasil, 1998. p. 93 – 148.
9. CREMA, S.; CAVALLI, M. SedInConnect: a stand-alone, free and open-source tool for the assessment of sediment connectivity. **Computers and Geosciences**, v. 111, p. 39–45, 2018. DOI: 10.1016/j.cageo.2017.10.009.
10. DRYFLOR et al. Plant diversity patterns in neotropical dry forests and their conservation implications. **Science**, v. 353, p. 1383-1387, 2016.
11. FERNANDES, M. F. et al. The Origins and Historical Assembly of the Brazilian Caatinga Seasonally Dry Tropical Forests. **Frontiers in Ecology and Evolution**, v. 10, 2022. DOI: 10.3389/fevo.2022.723286.
12. HALLEMA, D. W. et al. Regional patterns of postwildfire streamflow response in the Western United States: The importance of scale-specific connectivity. **Hydrological Processes**, v. 31, n. 14, p. 2582–2598, 2017. DOI: 10.1002/hyp.11208.
13. HASTENRATH, S. Exploring the climate problems of Brazil's Nordeste: A review. **Climatic Change**, v. 112, p. 243-251, 2012. DOI: 10.1007/s10584-011-0227-1.
14. HOOKE, J. Coarse sediment connectivity in river channel systems: A conceptual framework and methodology. **Geomorphology**, v. 56, n. 1–2, p. 79–94, 2003. DOI: 10.1016/S0169-555X(03)00047-3.

15. KEY, C. H.; BENSON, N. C. LA-1 Landscape Assessment (LA) Sampling and Analysis Methods. In: LUTES, D. C. et al. **FIREMON: Fire effects monitoring and inventory system**. Colorado: USDA Forest Service, 2005.
16. LIMA, N. E. DE et al. Characterization and biogeographical history of Neotropical dry ecosystems. **Rodriguésia**, v. 69, n. 4, p. 2209–2222, 2018a.
17. LÓPEZ-VICENTE, M.; GONZÁLEZ-ROMERO, J.; LUCAS-BORJA, M. E. Forest fire effects on sediment connectivity in headwater sub-catchments: Evaluation of indices performance. **Science of the Total Environment**, v. 732, 2020a.
18. LÓPEZ-VICENTE, M.; KRAMER, H.; KEESSTRA, S. Effectiveness of soil erosion barriers to reduce sediment connectivity at small basin scale in a fire-affected forest. **Journal of Environmental Management**, v. 278, 2021a.
19. LU, X. et al. Structural and sedimentological connectivity on a rilled hillslope. **Science of the Total Environment**, v. 655, p. 1479–1494, 2019. DOI: 10.1016/j.scitotenv.2018.11.137.
20. MARTÍNEZ-MURILLO, J. F.; LÓPEZ-VICENTE, M. Modelling hydrological connectivity in burned areas: A case study from South of Spain. **FLAMMA**, v. 7, n. 3, p. 5-9, 2016.
21. MARTÍNEZ-MURILLO, J. F.; LÓPEZ-VICENTE, M. Effect of Salvage Logging and Check Dams on Simulated Hydrological Connectivity in a Burned Area. **Land Degradation and Development**, v. 29, n. 3, p. 701–712, 2018. DOI: 10.1002/ldr.2735.
22. MARTINI, L. et al. Assessing the effect of fire severity on sediment connectivity in central Chile. **Science of the Total Environment**, v. 728, 2020. DOI: 10.1016/j.scitotenv.2020.139006.
23. MIDDLETON, N. J.; STERNBERG, T. Climate hazards in drylands: A review. **Earth-Science Reviews**, v. 126, p. 48-57, 2013. DOI: 10.1016/j.earscirev.2013.07.008.
24. MONTES-LEON, M. A. L. et al. National map of potential erosion. **Tecnologia y Ciencias del Agua**, v. 2, n. 1, p. 05-17, 2011.
25. NEMENS, D. G.; VARNER, J. M.; JOHNSON, M. C. **Environmental Effects of Postfire Logging: An Updated Literature Review and Annotated Bibliography**. Portland: USDA Forest Service, 2019. 35p. General Technical Report.
26. ORTÍZ-RODRÍGUEZ, A. J.; MUÑOZ-ROBLES, C.; BORSELLI, L. Changes in connectivity and hydrological efficiency following wildland fires in Sierra Madre Oriental, Mexico. **Science of the Total Environment**, v. 655, p. 112–128, 2019a.
27. PARKS, S. A.; DILLON, G. K.; MILLER, C. A new metric for quantifying burn severity: The relativized burn ratio. **Remote Sensing**, v. 6, n. 3, p. 1827–1844, 2014. DOI: 10.3390/rs6031827.
28. PHILLIPS, J. D. Synchronization and scale in geomorphic systems. **Geomorphology**, n. 137, p. 150-158, 2012. DOI: 10.1016/j.geomorph.2010.09.028.
29. REDIN, M. et al. Impacts of burning on chemical, physical, and biological soil attributes. **Ciência Florestal**, v. 21, n. 2, p. 381-392, 2011.
30. SACO, P. M.; WILGOOSE, G. R.; HANCOCK, G. R. Eco-geomorphology of banded vegetation patterns in arid and semiarid regions. **Hydrology and Earth System Sciences**, v. 11, p. 1717-1730, 2007. DOI: 10.5194/hess-11-1717-2007.
31. SAMPAIO, E. V. et al. Regeneration of Caatinga vegetation after cutting and burning in Serra Talhada, PE. **Pesquisa Agropecuária Brasileira**, v. 33, n. 5, 1998.
32. SANTANA, J. A. S. et al. Determination of critical periods for forest fires in the Seridó Ecological Station, Serra Negra do Norte-RN. **Revista Caatinga**, v. 24, n. 1, p. 43–47, 2011.
33. SOUZA, C. M. Jr. et al. Reconstructing three decades of land use and land cover changes in Brazilian biomes with Landsat archive and Earth Engine. **Remote Sensing**, v. 12, n. 17, p. 2735, 2020. DOI: 10.3390/rs12172735.
34. SOUZA, J. O. P. From environmental systems to the fluvial system - a review of concepts. **Caminhos de Geografia**, v. 14, n. 47, 2013.
35. SOUZA, J. O. P; ALMEIDA, J. D. M. Fluvial processes in drylands: a review. **Revista OKARA: Geografia em debate**, v. 9, n. 1, p. 108-122, 2015.
36. SOUZA, J.; HOOKE, J. Influence of seasonal vegetation dynamics on hydrological connectivity in tropical drylands. **Hydrological Processes**, v. 35, n. 11, 2021. DOI: 10.1002/hyp.14427.
37. SILVA, J. A.; PACHECO, A. DA P. Fire analysis in the caatinga environment from landsat-8 images, enhanced vegetation index and analysis by the main components. **Ciência Florestal**, v. 31, n. 1, p. 417–439, 2021. DOI: 10.5902/1980509843818.
38. STAVI, I. Wildfires in grasslands and shrublands: A review of impacts on vegetation, soil, hydrology, and geomorphology. **Water**, v. 11, n. 5, p. 1-20, 2019. DOI: 10.3390/w11051042.
39. TARCISIO, F. Natural regeneration of a Caatinga area in the Pernambuco hinterland, northeastern Brazil. **Cerne**, v. 19, n. 2, p. 229-235, 2013. DOI: 10.1590/S0104-77602013000200006.